



Figures and figure supplements

Neurovascular sequestration in paediatric *P. falciparum* malaria is visible clinically in the retina

Valentina Barrera et al

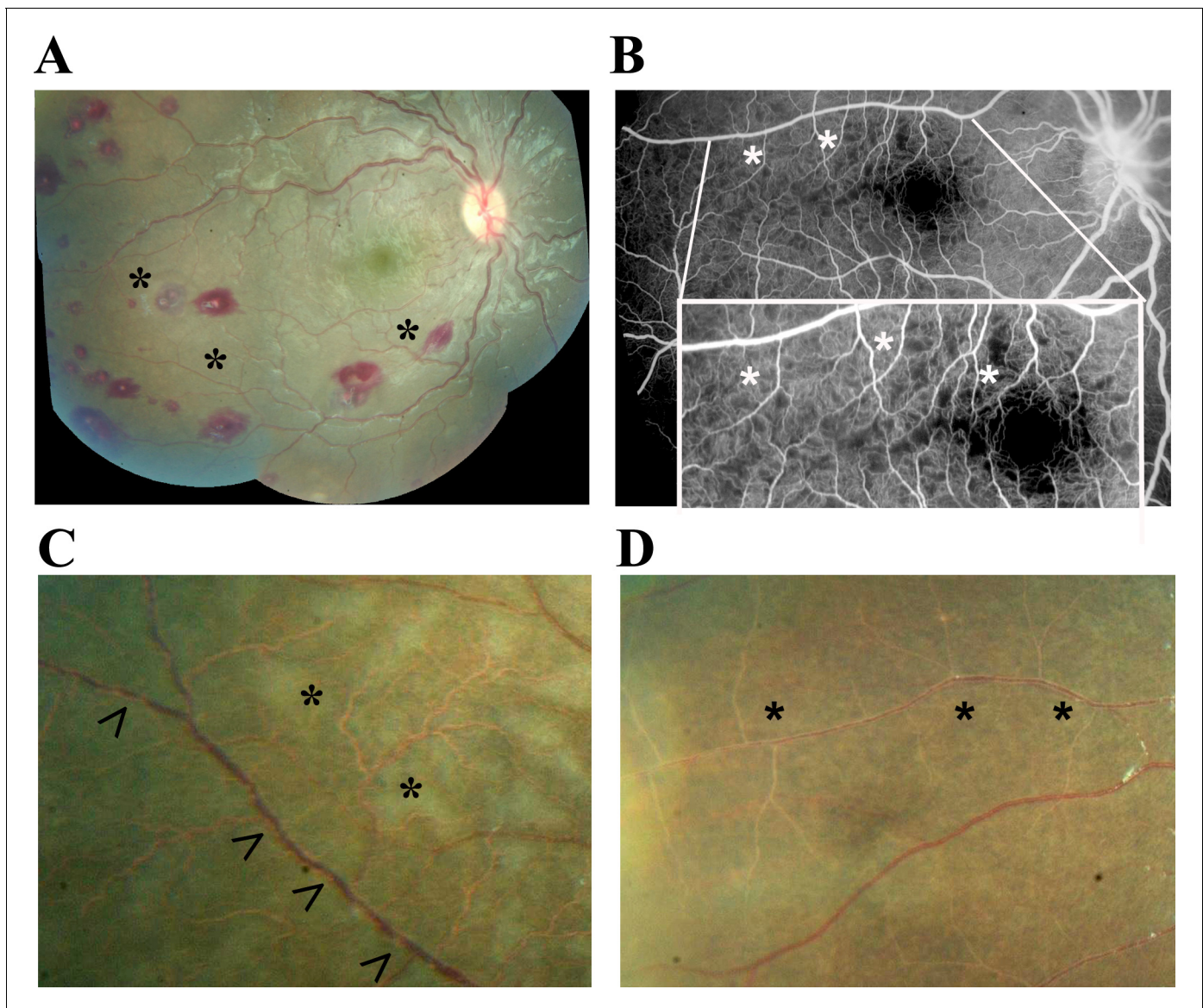


Figure 1. Principal features of malarial retinopathy (MR). (A) Montage image showing MR pathological features, including orange vessels (asterisks), white centred haemorrhages and whitening. (B) Corresponding fluorescein angiogram showing capillary nonperfusion (asterisks) mapping to retinal whitening. (C–D) Colour fundus image of retinopathy positive eyes (C, right; D, left eye; eyes were from different cases) showing orange intravascular material in large (arrowheads), small and postcapillary venules (asterisks), and capillaries; note retinal whitening also present.

DOI: <https://doi.org/10.7554/eLife.32208.002>

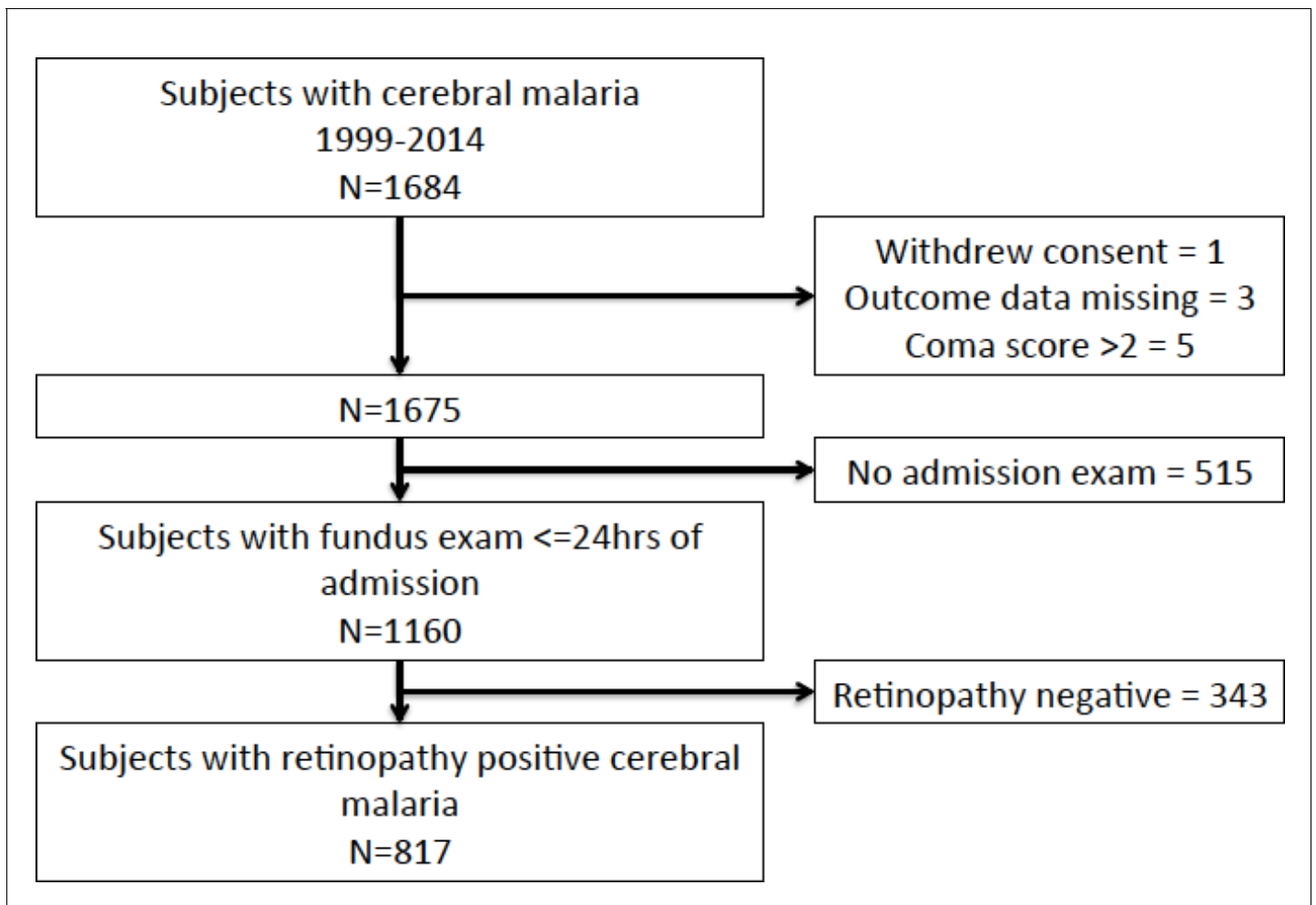


Figure 1—figure supplement 1. Flow chart describing clinical dataset.

DOI: <https://doi.org/10.7554/eLife.32208.003>

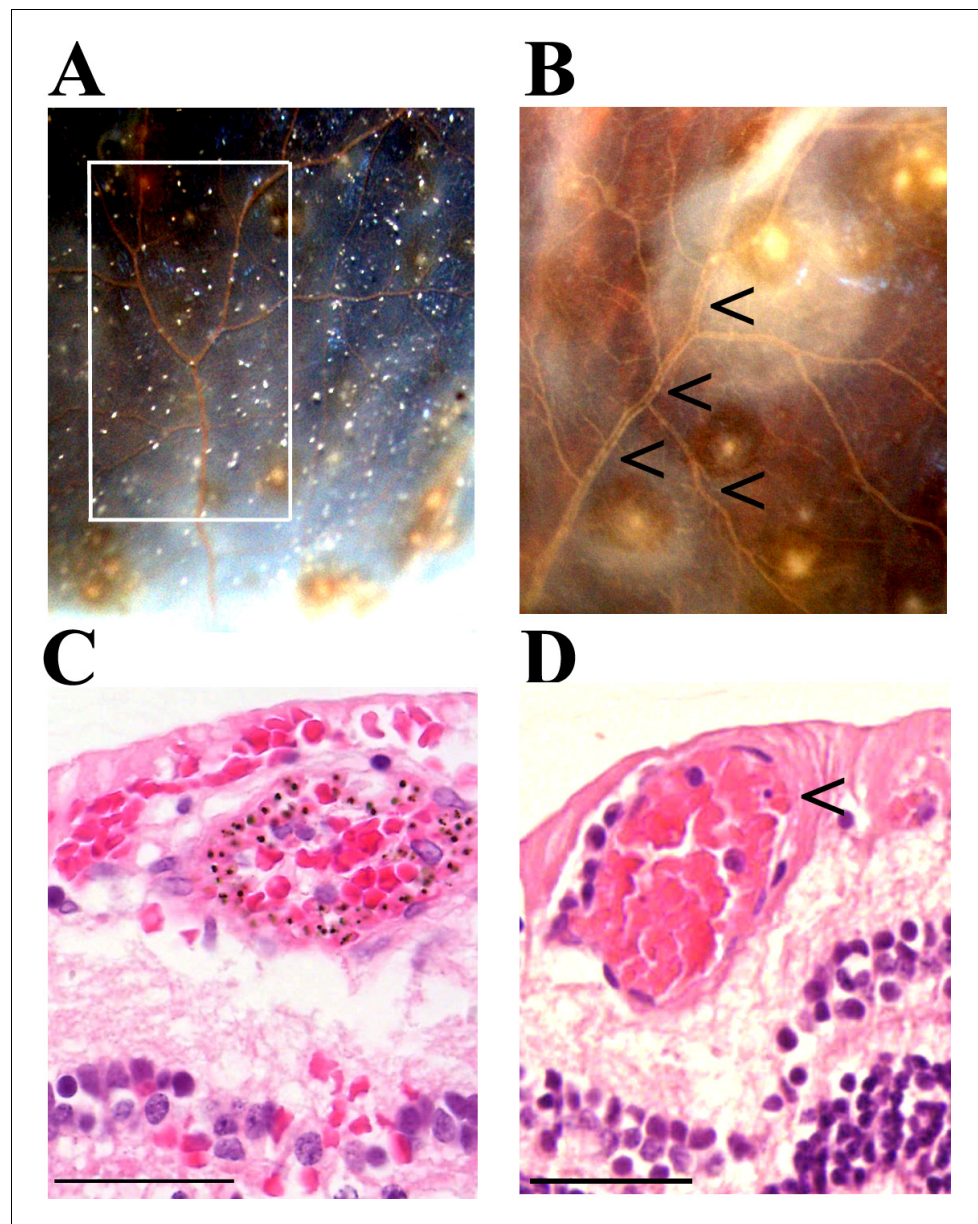


Figure 2. Vessel changes in malarial retinopathy. (A–B) Vessel colour changes (panels A–B) and intravascular filling defects (panel B, arrowheads) were identified during gross pathology examination (representative images of superior calotte and PO block from histology cases n. 5 and 7, respectively) N = 12. Abnormal vessels were sampled during gross pathology examination and analysed separately (see marked quadrant in panel A). (C–D) H and E staining of parasitised venules from MR cases sampled by punch biopsies from a retinal quadrant with (panel C shows the same orange vessel as in panel A) and without (panel D, case n. 15) vessel discolouration. (C) The margin of the vessel lumen has a near-complete layer of pigment-containing pRBCs (that stain less intensely pink than the adjacent non-parasitised RBC) on the endothelium. (D) Mild sequestration of pRBCs which is marked by an arrowhead. Scale bars (50 μ m, (C–D)).

DOI: <https://doi.org/10.7554/eLife.32208.007>

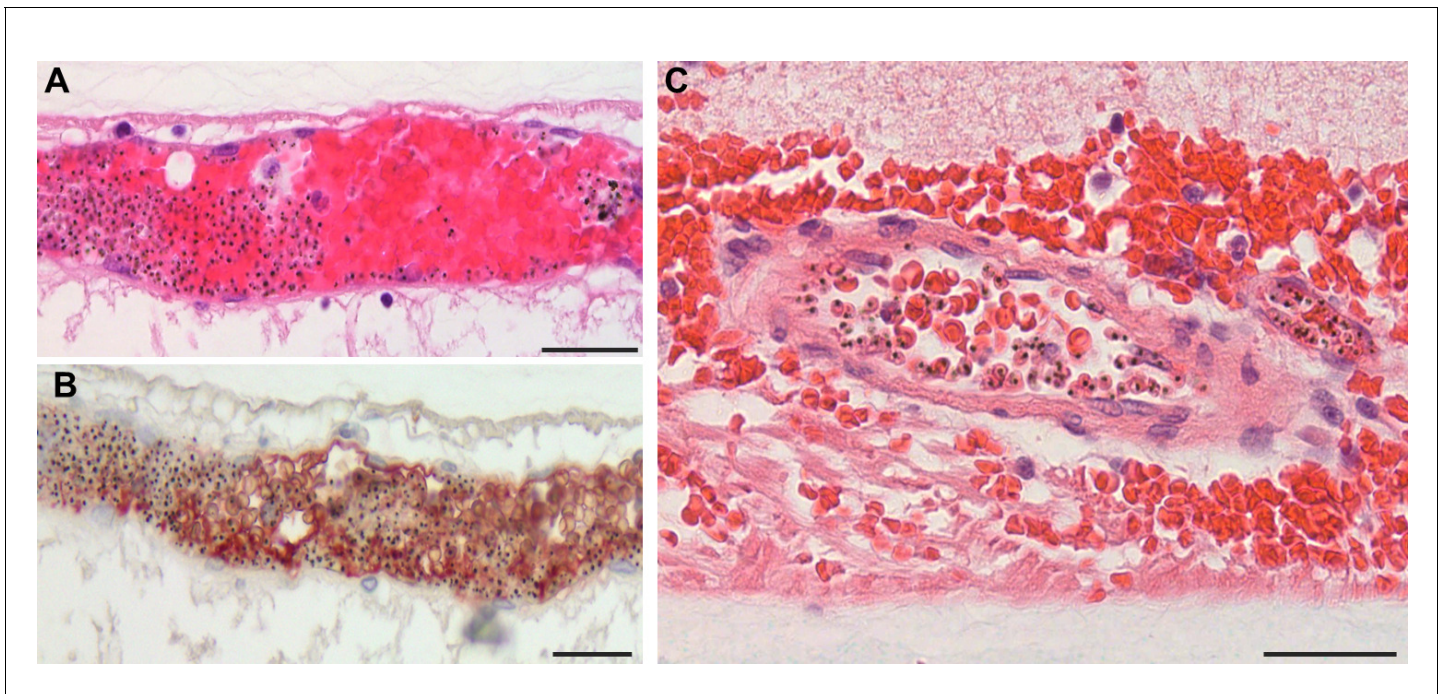


Figure 3. Severe pRBC sequestration in large venules and arterioles in MR with visible vessel discolouration. (A–B) Longitudinal section of large retinal venule from retinal area affected by intravascular filling defects on fluorescein angiography (histopathology case no. 9) analysed by H&E staining (A) and anti-fibrinogen IHC (B). Clusters of pRBC are seen within the vessel lumen and attached to the wall. (C) Cross section of a large retinal arteriole with moderate pRBC sequestration (case n. 5). Arteriole is surrounded by haemorrhage, probably of a venular origin as arteriolar vessel wall appeared intact (in multiple sections). Scale bars: 50 μ m (all panels).

DOI: <https://doi.org/10.7554/eLife.32208.008>

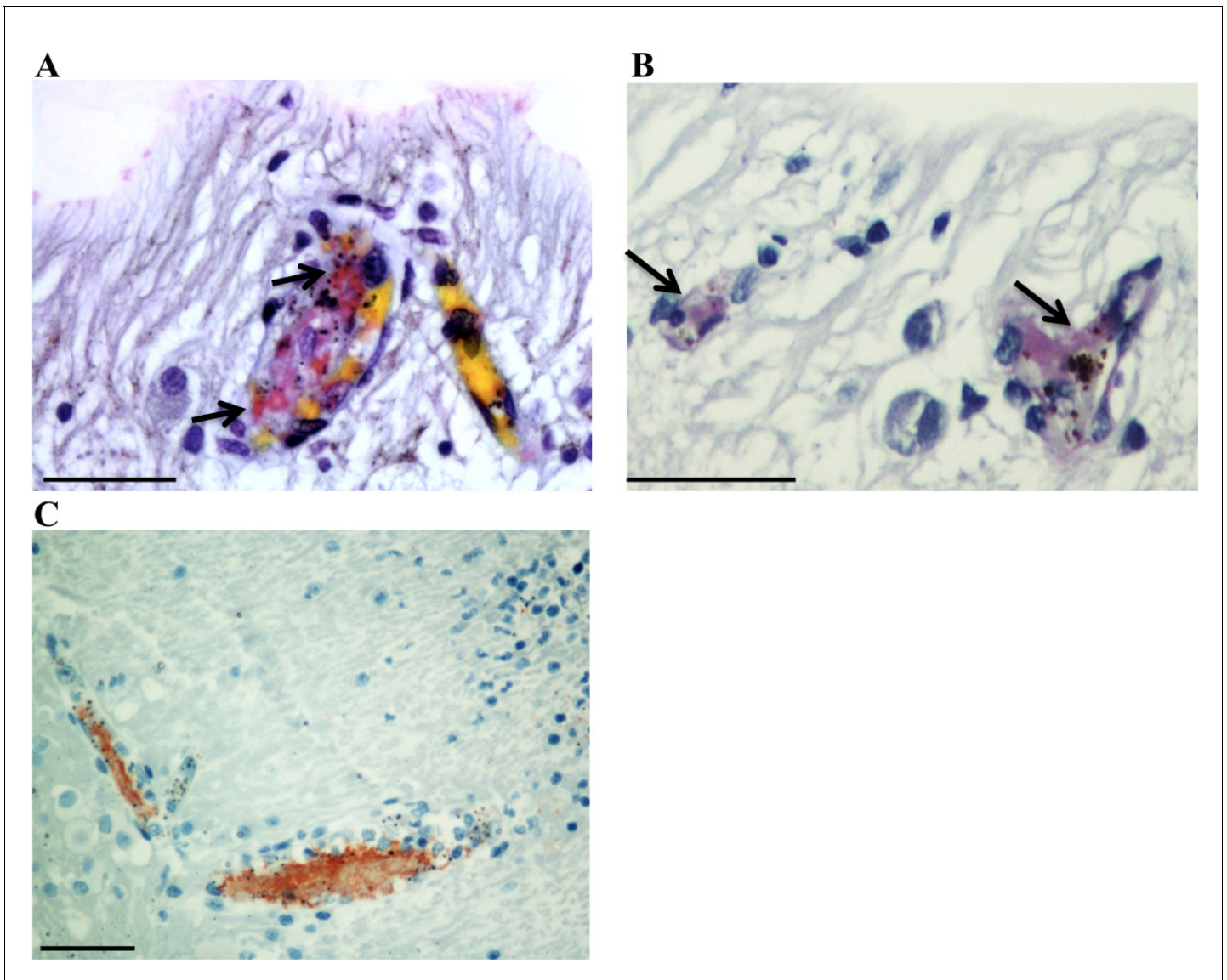


Figure 3—figure supplement 1. Detection of thrombi in post-mortem retinal periphery using a combination of MSB staining (panels A,B; arrows: intravascular thrombi are stained bright pink), and anti-CD61 platelet marker immunostaining (panel C, red stained). Scale bars: 50 μ m.

DOI: <https://doi.org/10.7554/eLife.32208.009>

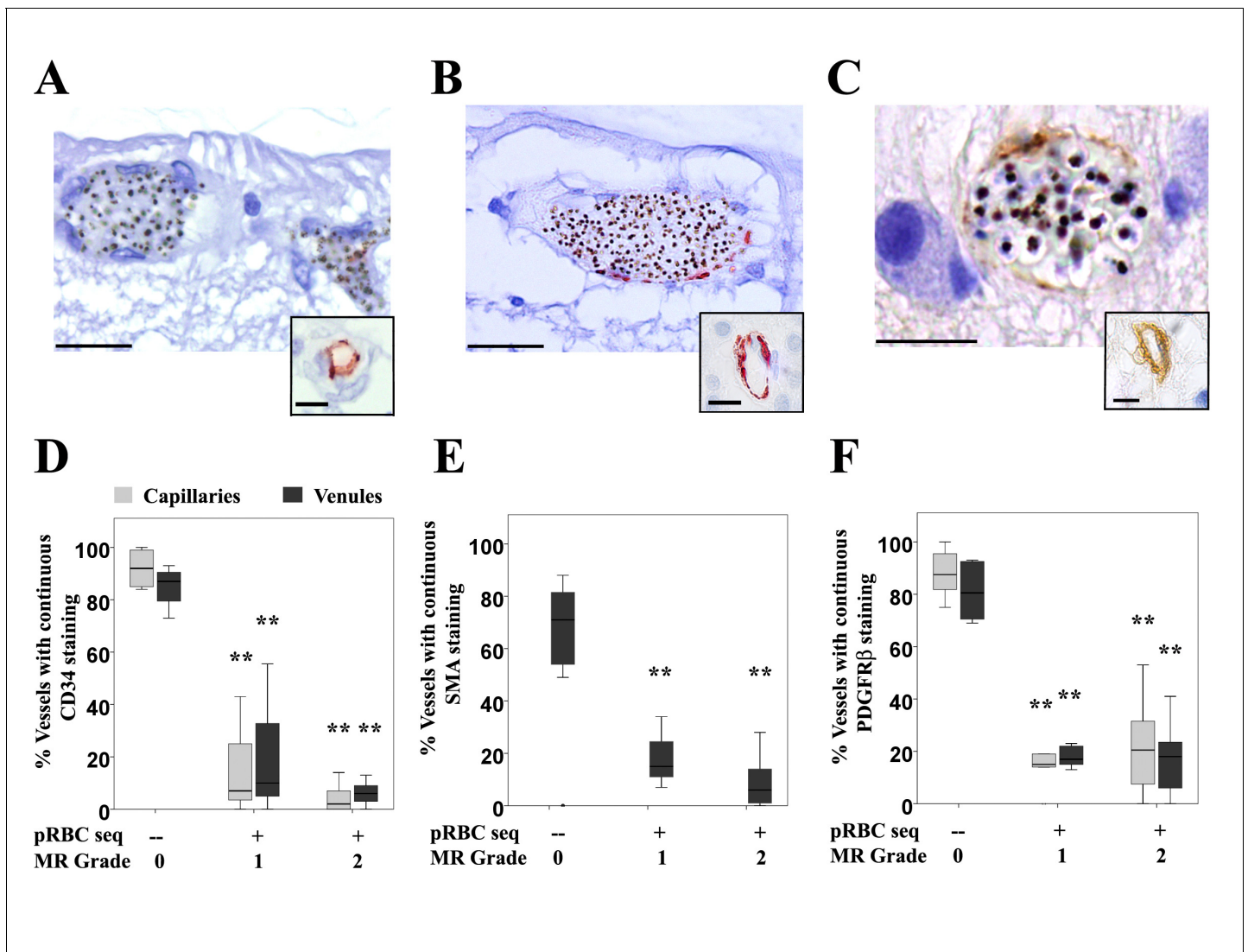


Figure 4. Vascular changes in retinal vessels in malarial retinopathy. (A–I) Expression of endothelial CD34 (panel A: case n. 3, inset: case n. 25 and D: box plot), pericytic SMA (panel B: case n. 12, inset: case n. 27 and E: box plot) and pericytic PDGFR β (panel C: case n. 13, inset: case n. 26 and F: box plot) markers. Insets show normal annular staining in absence of pRBC sequestration, whereas this annular pattern is lost in the sequestered vessels seen in A–C. SMA was only reported for venules as it does not produce an annular staining pattern in normal capillaries: panel E. N = 17 for CD34; N = 29 for SMA and PDGFR β immunostaining. ANOVA was used to compare means. ** $p < 0.005$. Scale bars: 20 μ m (A–C), 5 μ m (insets).

DOI: <https://doi.org/10.7554/eLife.32208.011>

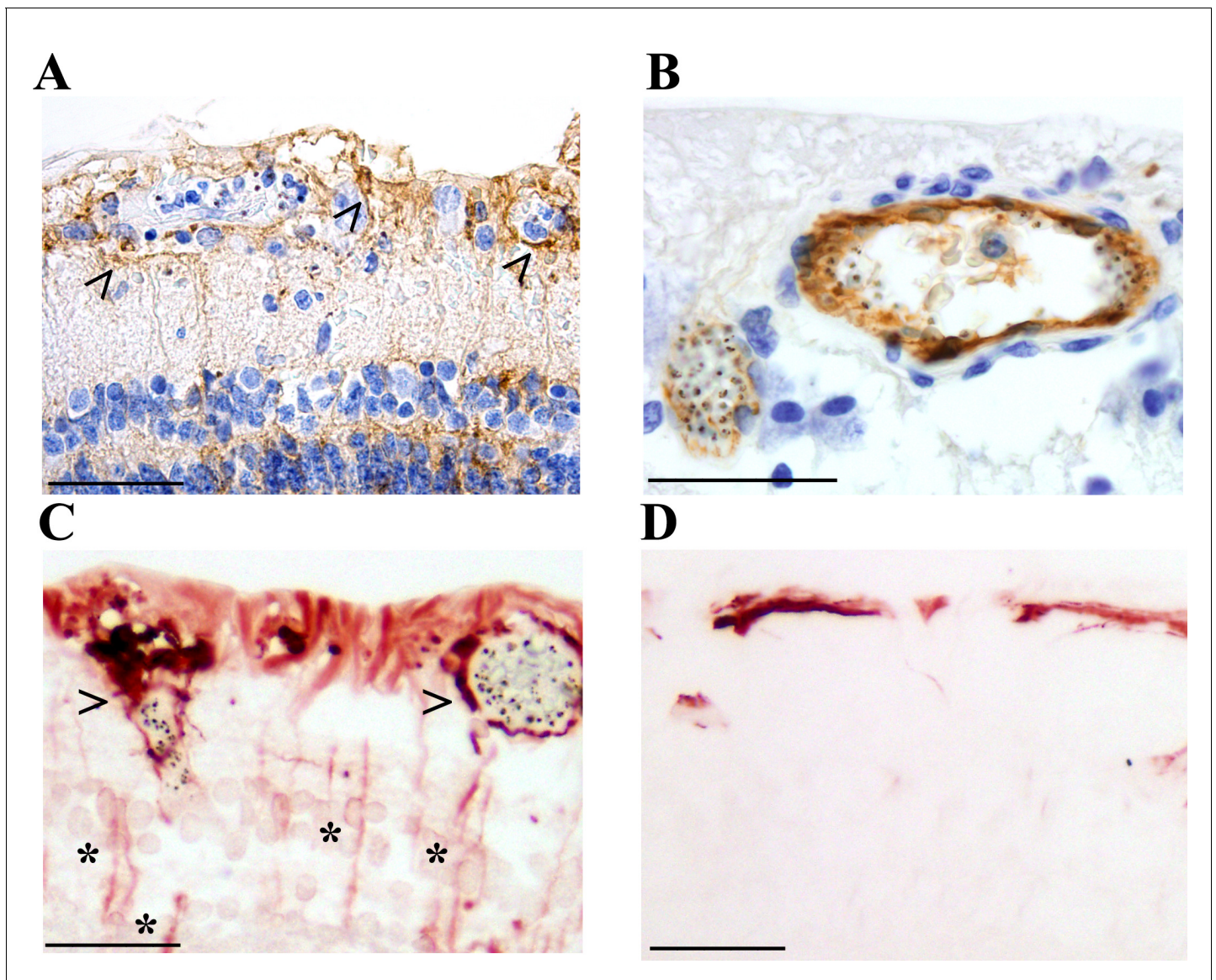


Figure 5. Activation of retinal glial cells in malarial retinopathy (MR). (A–B) Anti-ICAM-1 staining of MR-positive cases with (case n. 16, panel A) and without (case n. 13, panel B) vessel discolouration. Haematoxylin (blue) counterstain was used. (C–D) Anti-GFAP staining of orange-discoloured vessels in punch biopsy from MR-positive case n. 5, and in MR-negative case n. 25. Haematoxylin counterstaining was omitted here. In A and C, peri-vascular activated astrocytes and Müller cells are marked with arrowheads, and asterisks label Müller cell bodies. Scale bars: 50 μ m (all panels).

DOI: <https://doi.org/10.7554/eLife.32208.013>

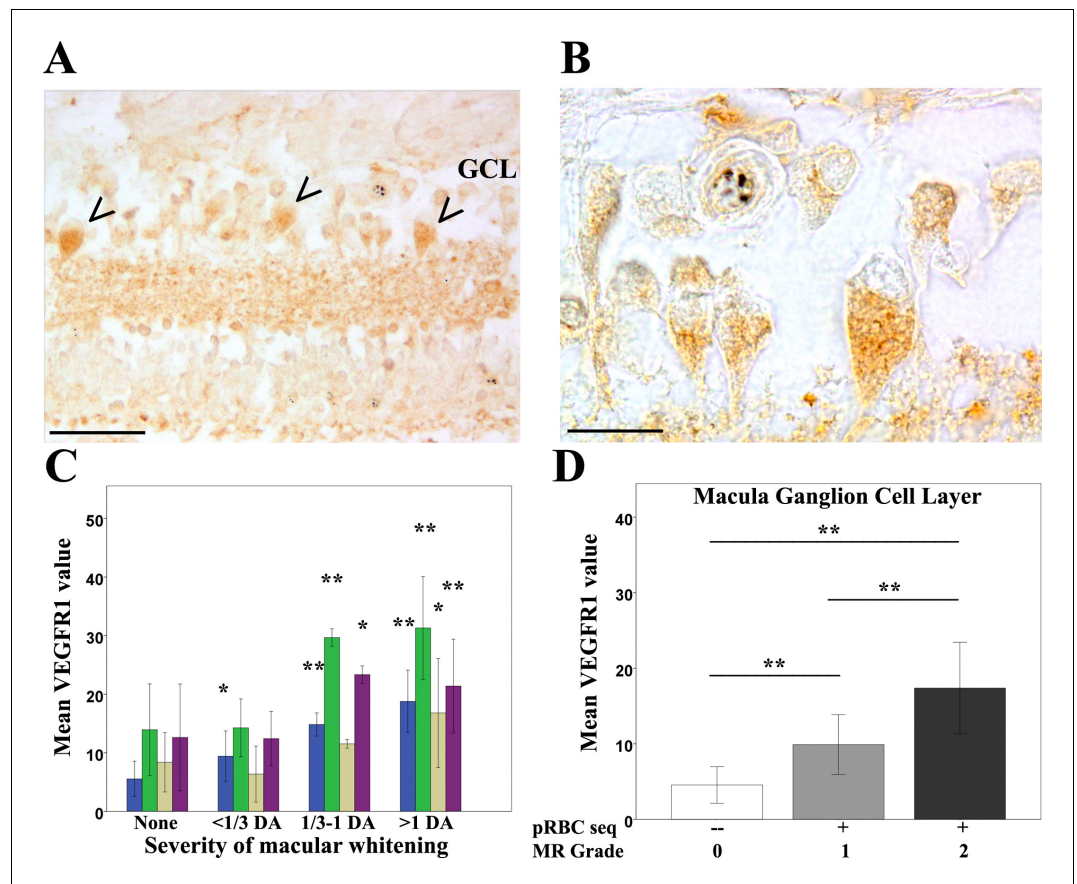


Figure 6. Clinicopathological association between retinal whitening in the macula and increased VEGFR1 expression in malarial retinopathy. (A–B) Immunostaining pattern in macula affected by whitening (case no 9) (low (A) and high (B) magnification; VEGFR1 +ve ganglion cell bodies indicated by arrowheads). (C) Cluster column chart showing densitometrically assessed intensity of immunoreactivity ('value') of VEGFR1 expression plotted by retinal layer against whitening severity, compared with MR –ve cases. Ganglion cell layer = GCL (blue); inner plexiform layer = IPL (green); inner nuclear layer = INL (light brown); outer plexiform layer = OPL (purple). (D) VEGFR1 levels in the GCL plotted against MR severity classification groups (grade 0 = none, 1 = mild, two moderate/severe). Means \pm SD are reported in both charts; ANOVA was used to compare means (N = 26). * $p \leq 0.05$ and ** $p \leq 0.001$. Scale bars: 50 μ m (panel A); 20 μ m (panel B).

DOI: <https://doi.org/10.7554/eLife.32208.014>

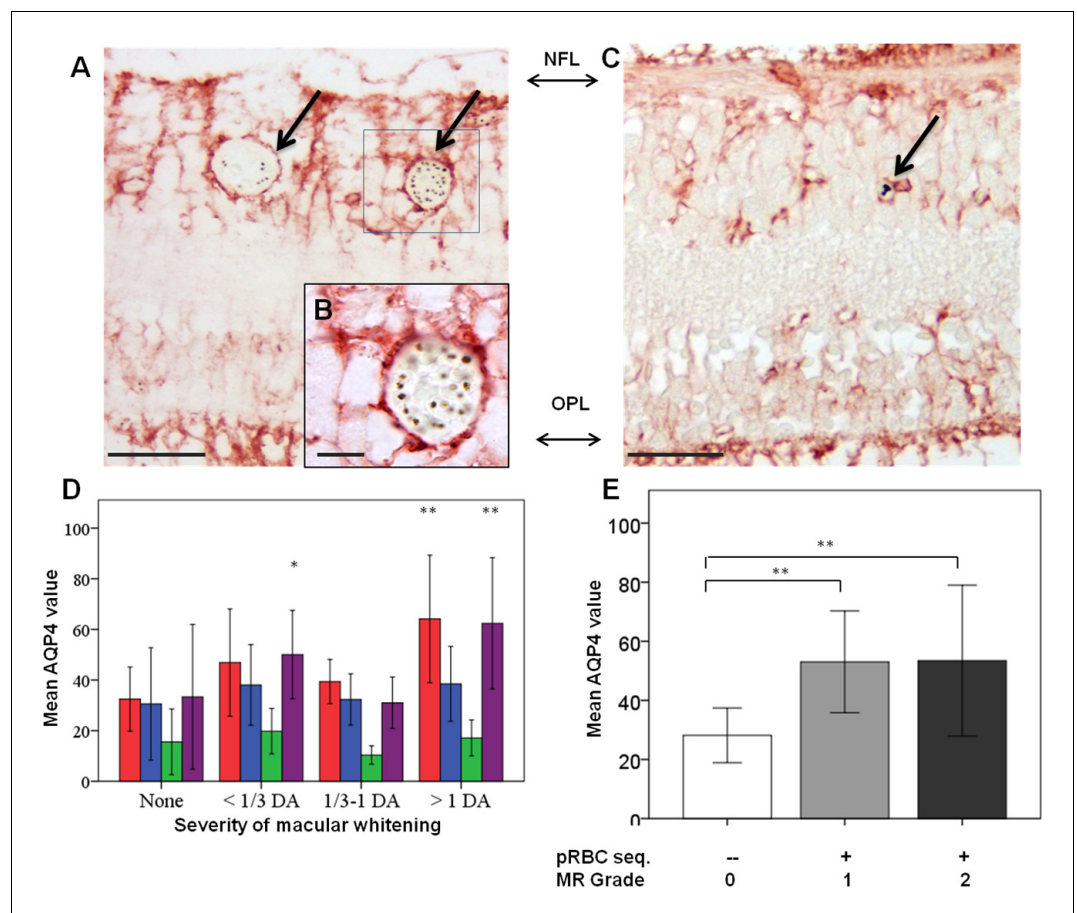


Figure 7. Clinicopathological association between retinal whitening in the macula and increased AQP4 expression in malarial retinopathy. (A–C) Immunostaining pattern in the macula with (A–B, case no 13) and without whitening (C, case no 21). Parasitised vessels are marked by arrows. The vertical linear pattern indicates Müller cell immunoreactivity for AQP4. (D) Cluster column chart showing densitometrically assessed intensity of immunoreactivity ('value') of AQP4 levels measured by IHC in the macula by retinal layers: nerve fibre layer = NFL (red), ganglion cell layer = GCL (blue), inner plexiform layer = IPL (green), outer plexiform layer = OPL (purple). (E): AQP4 levels in the nerve fibre layer plotted against MR severity classification groups (grade 0 = none, 1 = mild, two moderate/severe). Means \pm SD are reported in all graphs; ANOVA was used to compare means (N = 26). * $p < 0.05$ and ** $p < 0.001$. Scale bars: 50 μ m (panels C, E, F and G); 10 μ m (panel D).

DOI: <https://doi.org/10.7554/eLife.32208.016>

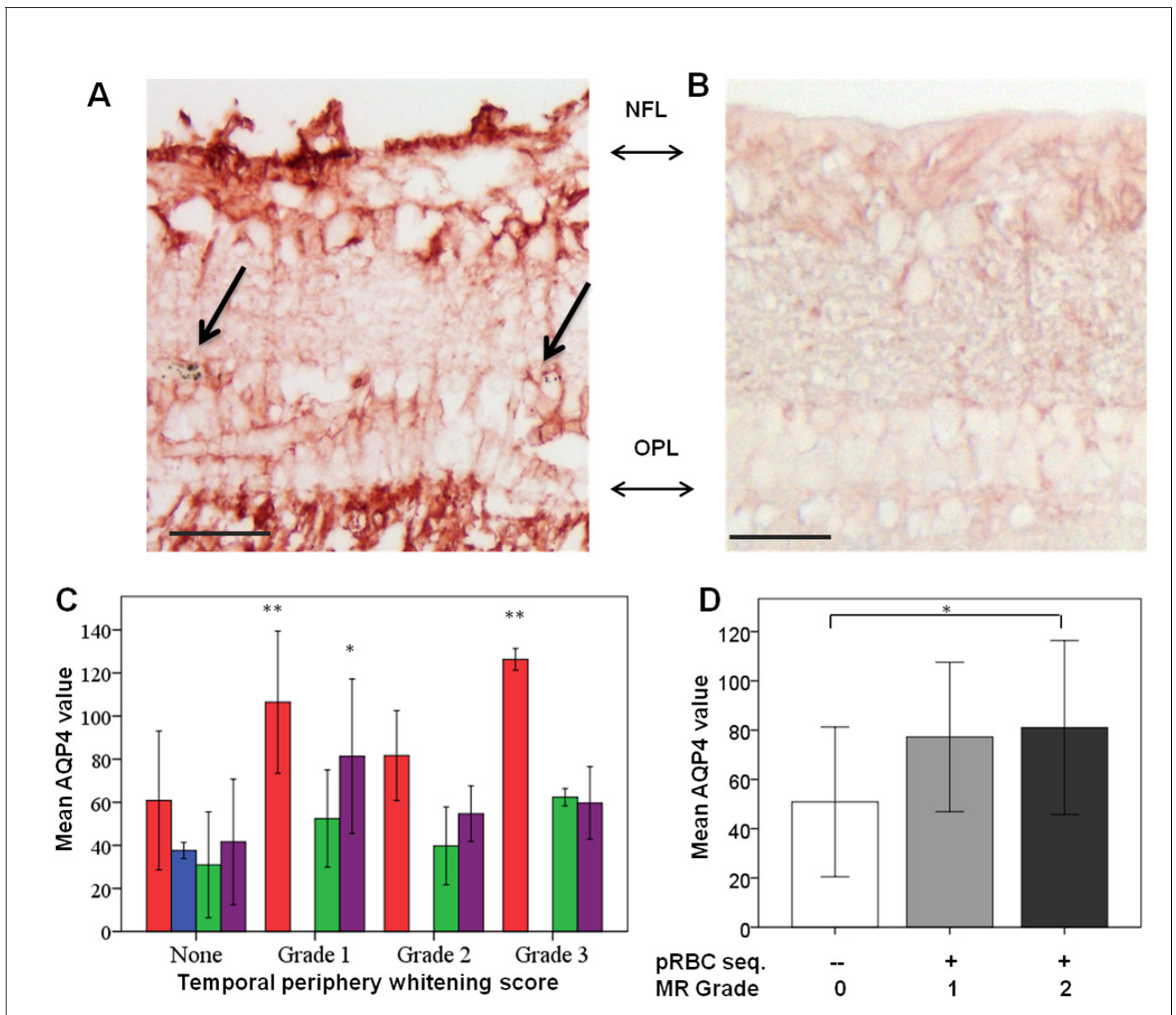


Figure 7—figure supplement 1. Clinicopathological association between retinal whitening in the peripheral retina and increased AQP4 expression in malarial retinopathy. (A–B) Immunostaining pattern is shown in MR-positive case with whitening (A, case n. 13) and MR-negative case (B, case n. 23). Parasitised vessels are marked by arrows. The vertical linear pattern indicates Müller cell immunoreactivity for AQP4. (C) Cluster column chart showing densitometrically assessed intensity of immunoreactivity ('value') of AQP4 levels measured by IHC in the peripheral retina by retinal layers: nerve fibre layer = NFL (red); ganglion cell layer = GCL (blue); inner plexiform layer = IPL (green); outer plexiform layer = OPL (purple). (D) AQP4 levels in the nerve fibre layer plotted against MR severity classification groups (grade 0 = none, 1 = mild, two moderate/severe). For details on grading zones see Appendix 2. Means \pm SD are reported in all graphs; ANOVA was used to compare means (N = 26). * $p \leq 0.05$ and ** $p \leq 0.001$. Scale bars: 50 μ m (panels A–B).

DOI: <https://doi.org/10.7554/eLife.32208.017>

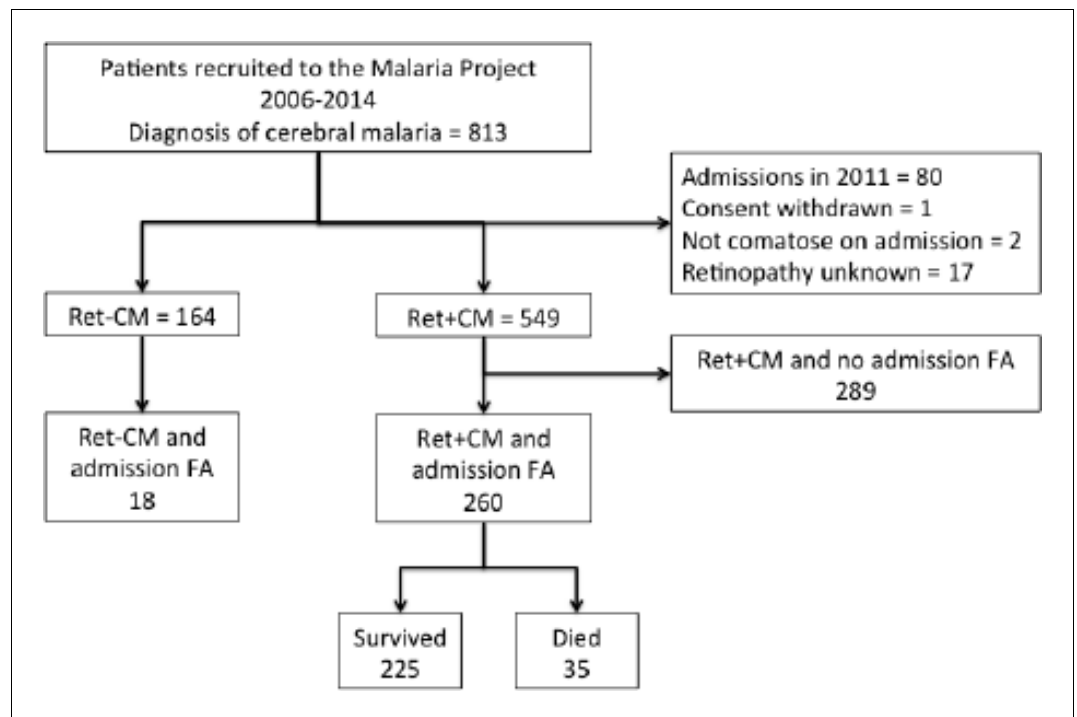


Figure 8. Flow chart describing fluorescein angiography dataset.

DOI: <https://doi.org/10.7554/eLife.32208.020>

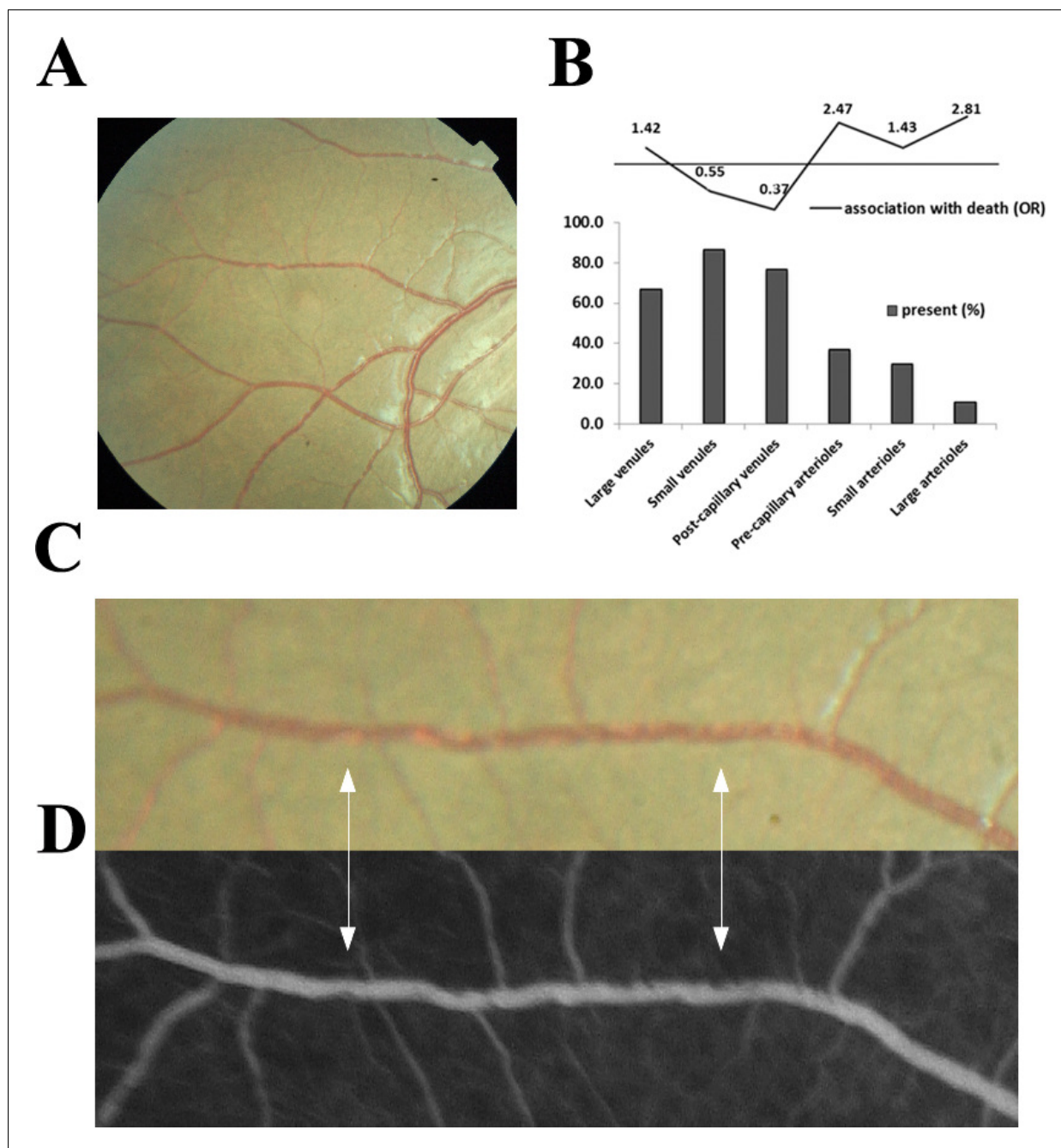


Figure 9. Visible sequestration in the retinal neurovasculature. (A–D): Orange intravascular material is seen in the retinal venule (A, C) which co-localises to the intravascular filling defects on fluorescein angiography (D) (see arrows). Chart (B) shows the frequency of visible sequestration in six microvessel types in 259 subjects with retinopathy +ve CM and the odds ratios of death within the admission.

DOI: <https://doi.org/10.7554/eLife.32208.021>

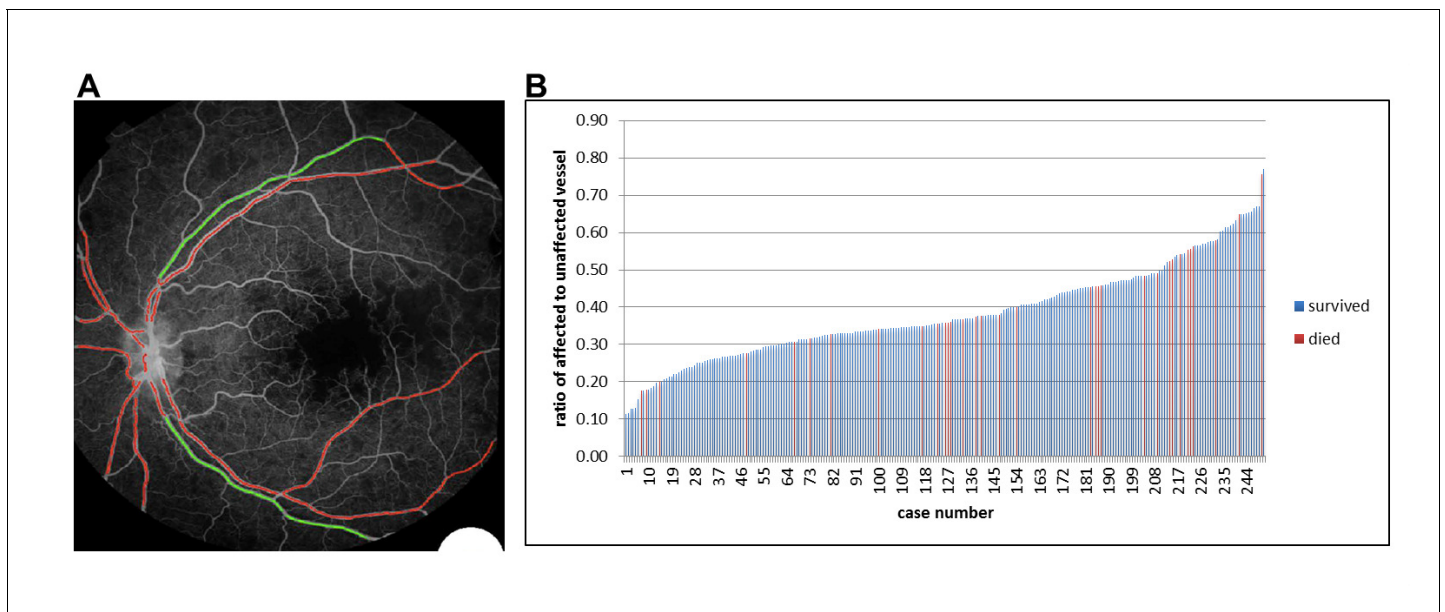
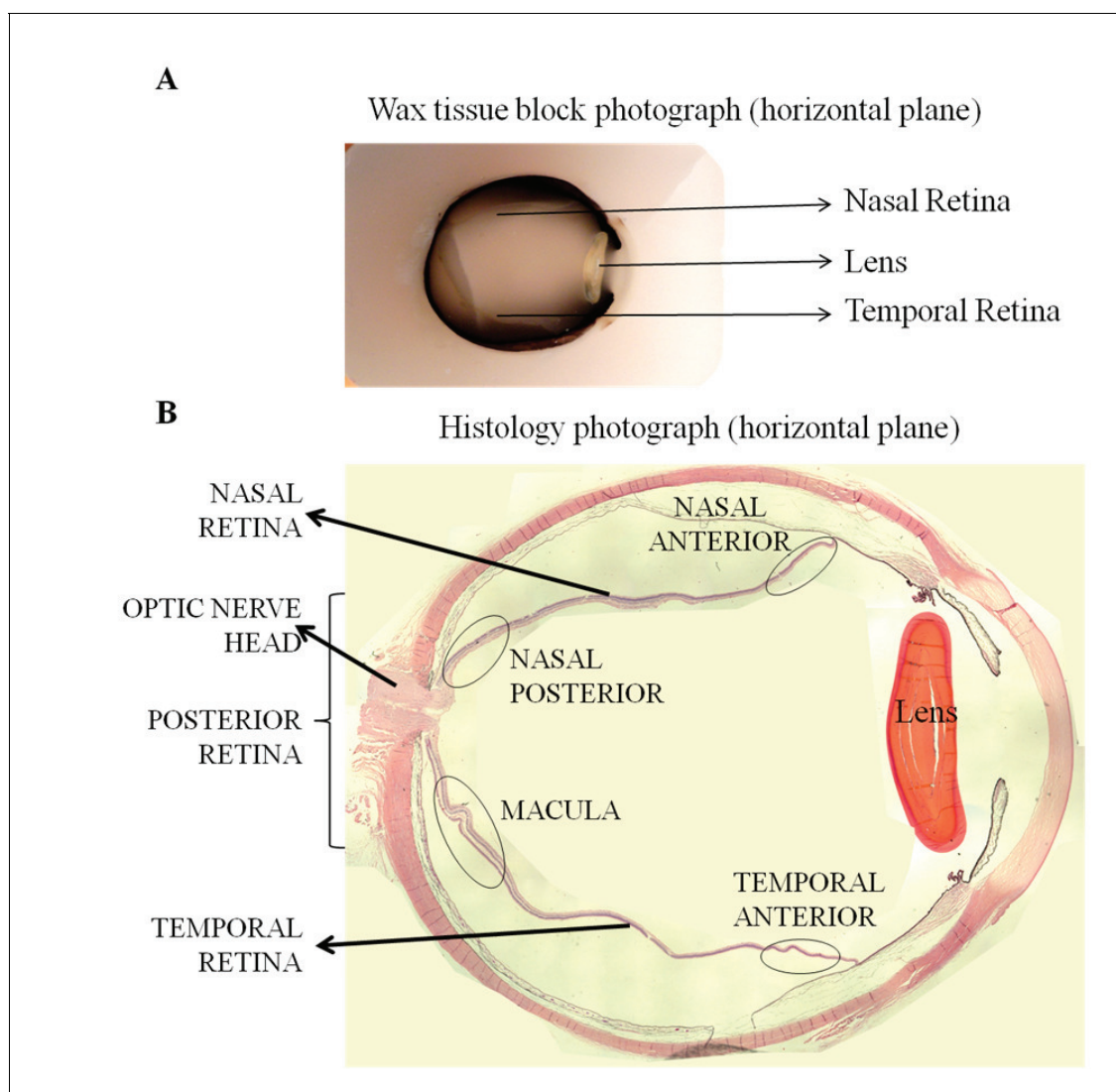


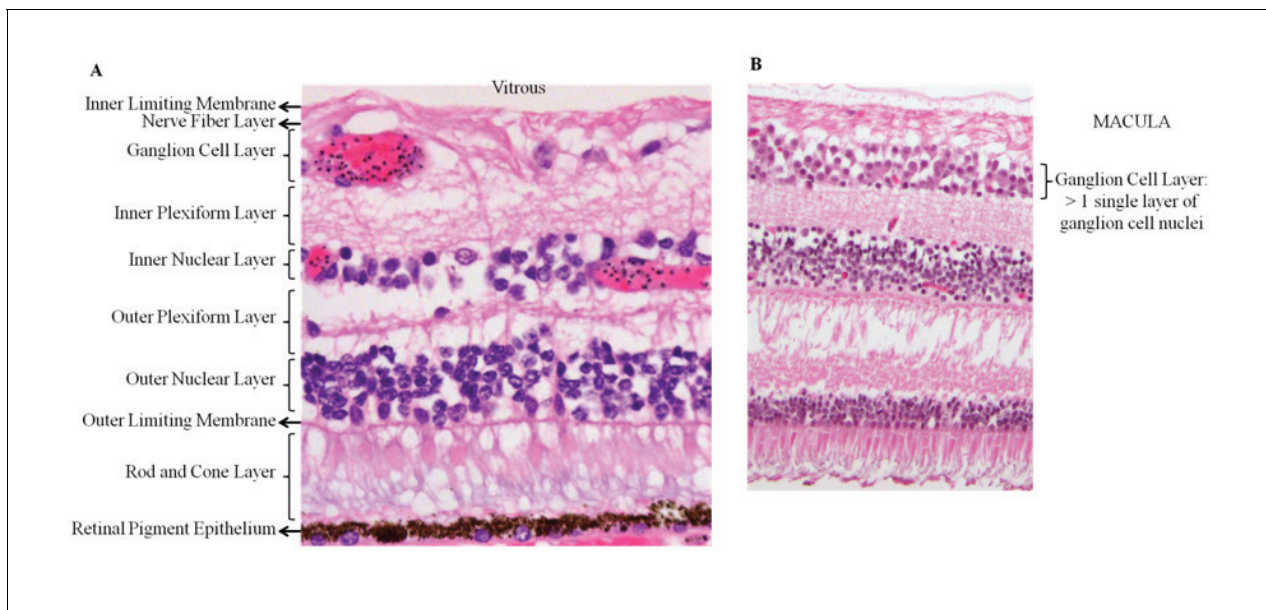
Figure 10. Semiautomated quantitative analysis of sequestration by length of affected vessel. (A) Example image of semiautomated system to show vessels affected by sequestration (red). (B) Chart showing distribution of proportion of detected vessel affected by sequestration related to survival in 251 eyes (one eye per case).

DOI: <https://doi.org/10.7554/eLife.32208.024>



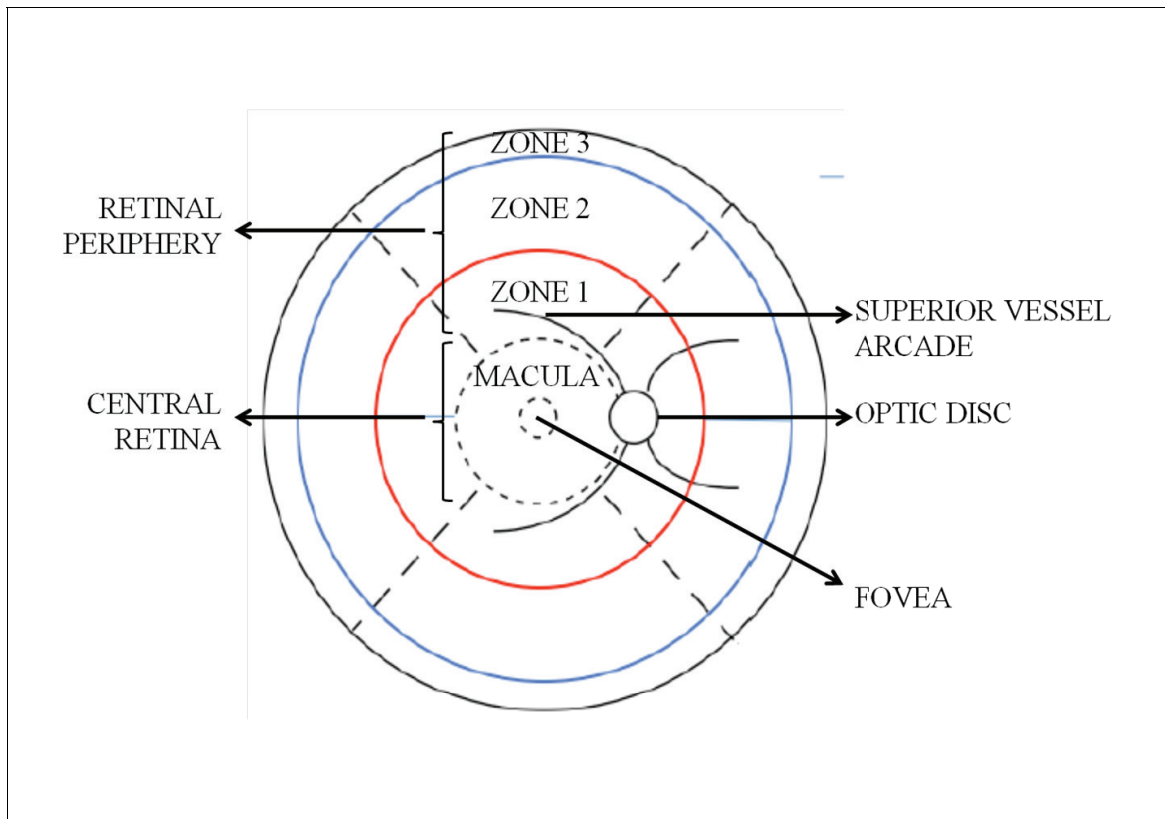
Appendix 1—figure 1. Orientation and topographical association in whole eye histology blocks (A) and in eye sections (B), used to perform correlation studies between fundal images and histology.

DOI: <https://doi.org/10.7554/eLife.32208.030>



Appendix 1—figure 2. Panel A: retinal structure on light microscopy (H&E staining). Panel B shows the specific feature of >1 cell thickness in the ganglion cell layer, used to identify the macula.

DOI: <https://doi.org/10.7554/eLife.32208.031>



Appendix 2—figure 1. Retinal zones used for clinical grading.

DOI: <https://doi.org/10.7554/eLife.32208.033>